ARTICLE

Highly Sensitive Flexible Pressure Sensors based on Graphene/Graphene Scrolls Multilayer Hybrid Films

Yi-heng Zhai[a], Tao Wang[b], Zhi-kai Qi[c], Xiang-hua Kong[a*], Hang-xun Xu[b*], Heng-xing Ji[c*]

a. School of Chemistry and Chemical Engineering, Hefei University of Technology, Hefei 230009, China
b. CAS Key Laboratory of Soft Matter Chemistry, Department of Polymer Science and Engineering, University of Science and Technology of China, Hefei 230026, China
c. Department of Applied Chemistry, CAS Key Laboratory of Materials for Energy Conversion, University of Science and Technology of China, Hefei 230026, China

(Dated: Received on July 30, 2019; Accepted on October 23, 2019)

In recent years, flexible pressure sensors have attracted much attention owing to their potential applications in motion detection and wearable electronics. As a result, important innovations have been reported in both conductive materials and the underlying substrates, which are the two crucial components of a pressure sensor. 1D materials like nanowires are being widely used as the conductive materials in flexible pressure sensors, but such sensors usually exhibit low performances mainly due to the lack of strong interfacial interactions between the substrates and 1D materials. In this paper, we report the use of graphene/graphene scrolls hybrid multilayers films as the conductive material and a microstructured polydimethylsiloxane substrate using *Epipremnum aureum* leaf as the template to fabricate highly sensitive pressure sensors. The 2D structure of graphene allows to strongly anchor the scrolls to ensure the improved adhesion between the highly conductive hybrid films and the patterned substrate. We attribute the increased sensitivity (3.5 kPa^{-1}), fast response time (<50 ms), and the good reproducibility during 1000 loading-unloading cycles of the pressure sensor to the synergistic effect between the 1D scrolls and 2D graphene films. Test results demonstrate that these sensors are promising for electronic skins and motion detection applications.

Key words: Pressure sensor, Graphene scrolls, Hybrid films, Electronic skins

I. INTRODUCTION

Flexible and wearable electronic devices are being developed for potential applications in electronic skins [1–3], biomedical monitors [4, 5], and motion detection [6–8]. In this context, materials with high flexibility that can be produced through low-cost processes are highly desired [9–16]. Currently available pressure sensors can be mainly classified into three different types: piezoelectric sensors [17–19], piezoresistive sensors [20–22], and capacitive sensors [23–25]. Piezoresistive sensors that show a change in resistance under applied pressure have been widely used owing to their many advantages, including ease of preparation, simple device structure, and convenient signal acquisition [26–28].

In general, a micro structured flexible substrate and a material with excellent conductivity are used in the fabrication of piezoresistive pressure sensors to optimize performance. With respect to the substrates, flexible substrates containing hemispheres arrays [29, 30], prism arrays [31], pyramid arrays [32, 33], and microgrooves [34] have been used in high-performance sensors. These microstructures are obtained by traditional lithography and often show good performance, but these processes are time-consuming in addition to being costly. Therefore, flexible substrates that can be made using simple low-cost preparation methods have been explored for the fabrication of high-sensitivity pressure sensors. For instance, Pang *et al.* [6] designed a pressure sensor with a sensitivity of 25.1 kPa^{-1} based on reduced graphene oxide (rGO) coated on a micro structured polydimethylsiloxane (PDMS) film with microroughness copied using an abrasive paper as a mold.

Apart from designing micro-structured substrates, it is also important to select a conductive material with high sensitivity to obtain pressure sensors with optimal performance. To date, conductive materials including carbon nanotubes (CNTs) [35, 36], carbonized nanofibers [37], graphene [38, 39], and metal nanoparticles [40] have been used in pressure sensors. Pan *et al.* [20] reported a hollow polypyrrole hydrogel-based pressure sensor with high sensitivity of 133.1 kPa^{-1} to

Authors to whom correspondence should be addressed. E-mail: kongxh@hfut.edu.cn, hxu@ustc.edu.cn, jihengx@ustc.edu.cn

detect pressure under 30 Pa. Sheng *et al.* [41] developed honeycomb-like graphene film-based pressure sensor decorated with bubbles on the surface, which showed ultrahigh sensitivity of 161.6 kPa^{-1}. Metal nanowires have been commonly used as the conductive material in flexible pressure sensors. However, the interface between the substrate and the 1D material, such as a nanowire, is not strong enough, resulting in low sensitivity of the sensor [42]. For example, He *et al.* [43] reported polypyrrole/silver coaxial nanowire aero-sponge with a sensitivity of only 0.33 kPa^{-1}. In this context, a 2D material, such as a graphene film, can serve as both a conductive contact and as a support for the 1D conductor, thereby increasing contacting area with the substrate [44]. Therefore, we believe that the synergistic effects between the two constituent components in a 1D-2D hybrid film can be potentially attractive for pressure sensors.

An optimal conductive material should be interconnected to form a continuous electron pathway, deformable in shape and variable in conductivity with the pressure, and robust under repeated pressure loading/unloading. In this paper, we report a high-performance flexible pressure sensor based on graphene/graphene scrolls (G/GS) hybrid films as the conductive material and using micro-structured PDMS (m-PDMS) replicated from *Epipremnum aureum* leaf as the flexible substrate. The unique composite structure combining G with GS, both of which are prepared by chemical vapor deposition (CVD) followed by simple etching, allowing to significantly improve performance of the pressure sensor. The substrate m-PDMS with its hierarchical microstructure copied from leaves also plays an important role in achieving high performance. The obtained pressure sensor shows high sensitivity (3.5 kPa^{-1}), fast response time (<50 ms), and good reproducibility during >1000 loading-unloading cycles. We have also tested the applications of the G/GS pressure sensor for human motion detection based on its response to periodic stress and bending force to demonstrate its potential application in smart wearable devices.

II. EXPERIMENTS

A. Structure characterization

Optical microscopy (Leica DM2500M) and scanning electron microscopy (SEM, FEI Apreo) were used to study the morphology and structure of the samples. Raman spectra were recorded using Renishaw inVia micro Raman spectrometer with a 50× objective lens and a 532 nm laser as the excitation source.

B. Mechanical properties measurements

A compression performance testing system (UTM 2000) was used to apply pressure and a precision LCR meter (TH2827A) was used to characterize the electrical properties and to record the electrical response of the pressure sensor.

III. RESULTS AND DISCUSSION

A. Fabrication of the G/GS/m-PDMS pressure sensor

Single-layer graphene was prepared by CVD (see details in supplementary materials). To transfer graphene, we spin-coated a thin layer of polymethylmethacrylate (PMMA) on one side of the graphene layer (which we called top graphene) forming a PMMA/top graphene/Cu foil/bottom graphene structure. Next, the PMMA/top graphene/Cu foil/bottom graphene was floated on $(NH_4)_2S_2O_8$ solution to etch Cu. During Cu foil etching, the unprotected bottom-side graphene invariably developed cracks and defects that allow the etchant to penetrate through. Due to surface tension, the released graphene domains rolled up into scrolls and attached onto the top-G/PMMA films [45]. After the Cu was removed, the PMMA layer was dissolved with acetone to form graphene/graphene scrolls (G/GS) hybrid films, which we denote here as 1-layer G/GS hybrid films. The G/GS films can be transferred to essentially any other substrates. By repeating the transfer process, 2-, 3-, or 4-layer G/GS films can be obtained as shown in FIG. 1(a−c). For micro-structuring the substrate, we used a leaf of the common indoor plant, *Epipremnum aureum*. After cutting and cleaning, the leaf was placed on a 2.2 cm×2.2 cm glass slide. The PDMS (Sylgard 184, Dow Corning) was prepared by mixing the base and curing agent in the weight ratio 10:1 [46]. The uncured PDMS was spread on the leaf-covered glass sheet by adding it dropwise onto the leaf to completely cover the sheet. After heating at 60 °C for 8 h, the excess PDMS was scraped off with a blade, leaving m-PDMS substrate to replicate the microstructure of the leaf fragment. The presence of a large number of sharp ridges significantly increased surface roughness and provided a large number of contact points which contributed to improving the performance of the pressure sensor [42]. The G/GS film of different layer numbers were transferred onto the m-PDMS substrate to serve as the conductive material for the pressure sensor (FIG. 1(d)). Silver paste was coated on one side of each G/GS film to which, copper electrodes were attached (FIG. 1(e)). The schematic diagram of the working mechanism is shown in FIG. 1(f).

The distribution of graphene scrolls in the hybrid film was studied from optical microscopy images. The scrolls are randomly distributed over the surface, and their in-plane density increases with the number of stacked G/GS layers. FIG. 2(a−e) show that the percentage area covered by 1, 2, 3, and 4-layer graphene scrolls are (7.87±1.84)%, (16.22±1.65)%, (25.02±1.52)%, and (30.37±1.13)%, respectively (see statistical methods in supplementary materials). Individual G/GS films can

DOI:10.1063/1674-0068/cjcp1907146

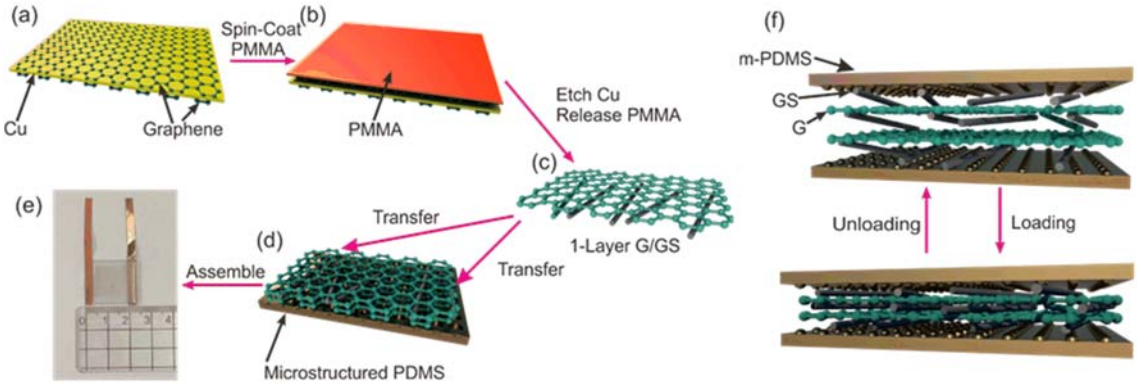

FIG. 1 Fabrication of G/GS pressure sensor. (a−c) Fabrication of G/GS films of different layers. (d) PDMS substrate with microstructures on surface that replicates the surface structure of *Epipremnum aureum* leaf coated with G/GS films. (e) Photograph of a G/GS pressure sensor assembled using m-PDMS and G/GS films. (f) Schematic of the structure deformation when pressure is loading/unloading.

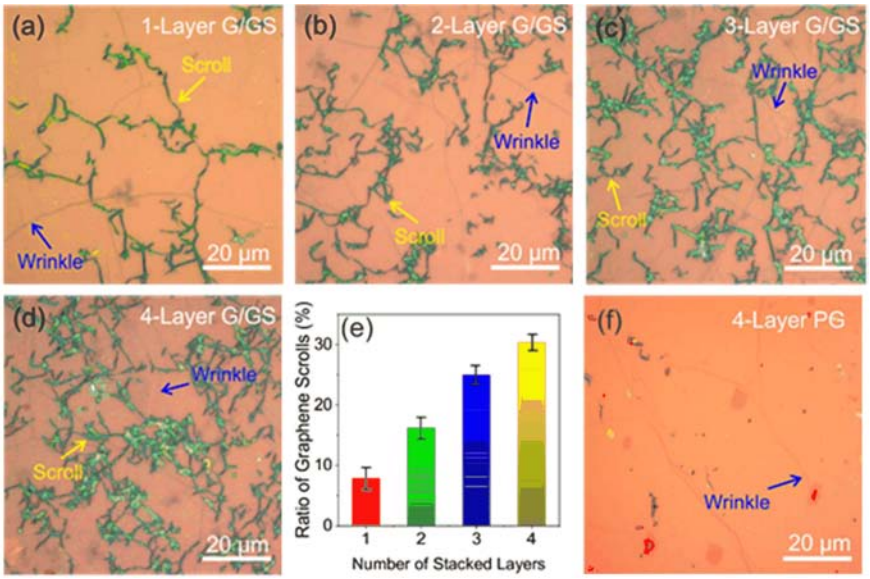

FIG. 2 Structure of the G/GS films. (a−d) Optical micrographs of 1-, 2-, 3-, and 4-layer G/GS films. (e) The fraction of the area covered by graphene scrolls in hybrid films with different number of stacked layers. (f) Optical micrographs of 4-layer PG films.

be transferred to m-PDMS substrates to conformally coat the micro-structured surface. The hybrid films were further characterized by Raman spectroscopy. FIG. S1 (supplementary materials) shows Raman spectra taken from two areas on a hybrid film. Both spectra show no D band (∼1350 cm^{-1}) confirming the high quality of the graphene films. Besides, I_{2D}/I_G ratio and the full width at half-maximum of the 2D band confirm the multilayer structure of the hybrid films. The SEM image of m-PDMS coated with G/GS films shows clearly that the presence graphene enables the G/GS films to make better contact with the m-PDMS substrate and the composite films closely adhere to the micro-structured surface (FIG. S2 in supplementary materials). In addition, the optical micrographs of 4-layer PG films are shown in FIG. 2(f). The conformal coating and good adhesion of G/GS films on the m-PDMS substrate provide excellent conditions for the testing of pressure sensors.

B. Performance of the G/GS pressure sensor

Sensitivity is one of the most important parameters of a pressure sensor. Mathematically, sensitivity can be expressed as $S=(\Delta R/R_0)/\Delta P$, where $\Delta R/R_0$ is the relative change in resistance and ΔP is the change in pressure [47]. Even though all the sensors tested in this study use graphene films as the conductive material, 4-, 3-, and 2-layer GS/G pressure sensors show different S

DOI:10.1063/1674-0068/cjcp1907146

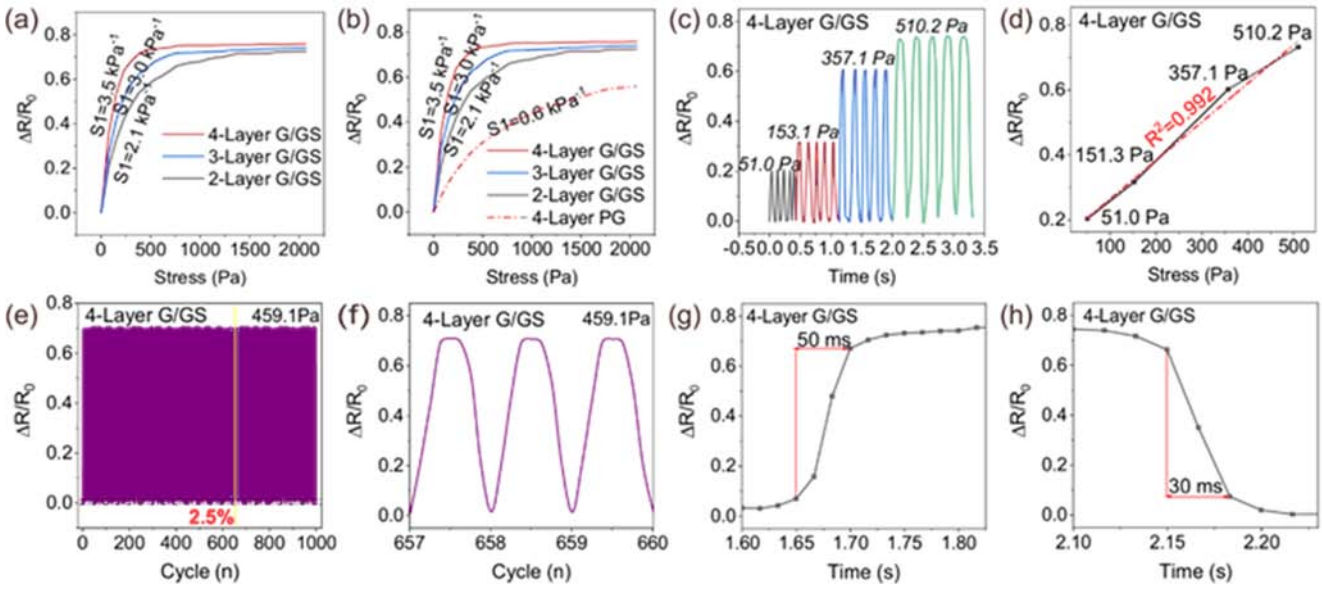

FIG. 3 Electromechanical properties of the G/GS pressure sensor. (a) Sensitivity of G/GS pressure sensors with different numbers of stacked G/GS layers. (b) Sensitivity of the pressure sensor in the presence of graphene scrolls compared to that of pure graphene film. (c) Response of the pressure sensor under different stress conditions. (d) Linear relationship between $\Delta R/R_0$ and stress. (e) Performance of the pressure sensor during 1000 cycles under 459.1 Pa pressure. (f) Magnified image of (e). Response time of (g) 50 ms and (h) 30 ms for the 4-layer G/GS pressure sensor.

values of 3.5, 3.0, and 2.1 kPa^{-1} (FIG. 3(a)), in the pressure range of 0−0.45, 0−0.75, and 0−1.30 kPa, respectively.

We attribute the different performances of the G/GS pressure sensors with different number of G/GS layers to the presence of graphene scrolls. In the initial state, G/GS films are contacted to each other, forming conductive pathways. When the pressure is applied, a greater number of scrolls bridge the bilevel monolayer graphene to form a percolating conducting network (FIG. 1(f)), resulting in gradual decrease in resistances. Meanwhile, the scrolls also prevent contact between layers, leading to a highly resistive initial configuration when no pressure is applied on the sensor. Under applied pressure, the contact area of the scrolls increases dramatically and the resistance of the pressure sensor rapidly decreases, leading to the high sensitivity. This also accounts for the highest sensitivity obtained for the 4-layer G/GS pressure sensor. To further compare the performance of the sensors in the presence and absence of scrolls and its impact on the sensitivity, we also tested a pressure sensor with 4-layer PG (pure graphene) films; as shown in FIG. 3(b), the sensitivity S is measured to be 0.6 kPa^{-1}. This result highlights the significant difference in sensitivity in the presence of scrolls. Furthermore, we list the recently reported piezoresistive with general 1D materials sensors from previous work (Table S1 in supplementary materials).

The results described above have confirmed the key role of scrolls in maintaining high sensitivity by forming a conductive bridge between the two layers of monolayer graphene. To test the stability of the sensor under repeated application of pressure, we have tested its response and repeatability. We applied a dynamic pressure cycle of 51.1, 153.1, 357.1, and 510.2 Pa on a 4-layer G/GS pressure sensor. As seen in FIG. 3(c), the response of the pressure sensor is both stable and reproducible. Moreover, the observed change in $\Delta R/R_0$ under dynamic cyclic pressure of different magnitudes is consistent with the change in sensitivity described in FIG. 3(a). Furthermore, the slope of the linearity range determines the sensitivity, while the length of the linearity range determines the detection limit of the pressure sensor. In our work, we tested the 4-layer G/GS pressure sensor at 51.1, 153.1, 357.1, and 510.2 Pa for 50 cycles, and the average of the maximum $\Delta R/R_0$ value at each pressure was calculated. This average was then plotted against stress. A linear relationship (R^2=0.992) is obtained as shown in FIG. 3(d).

FIG. 3(e) describes results of the repeatability testing for 4-layer G/GS pressure sensor during 1000 cycles at 459.1 Pa. As can be seen from FIG. 3(e), the pressure sensor maintains a high signal-to-noise ratio [48] and the change in $\Delta R/R_0$ is within 2.5% after 1000 loading-unloading cycles; the magnified plot covering cycle numbers from 657 to 660 shown in FIG. 3(f) confirms that the pressure sensor has good reproducibility under repeated application of pressures and the graphene scrolls remain stable under these conditions. We also measured the response time of the sensors to 2.0 kPa pressure; the response time is within 50 ms for the 4-layer G/GS pressure sensor (FIG. 3(g, h)). The response time of the 3-, and 2-layer G/GS pressure is within 95 and 175 ms, respectively (FIG. S3 in supplementary materials).

DOI:10.1063/1674-0068/cjcp1907146

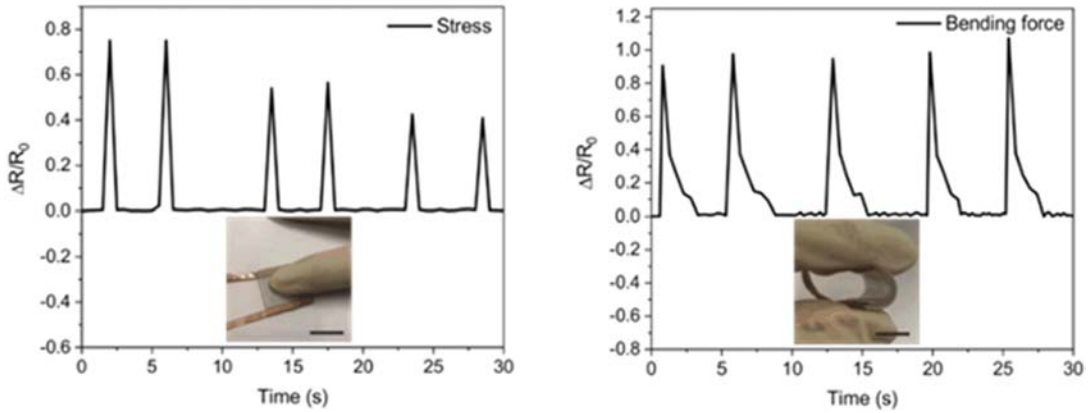

FIG. 4 Artificial stress and bending monitoring. Scale bar of the insets is 10 cm.

C. Artificial stress and bending monitoring

The G/GS pressure sensor for artificial stress and bending monitoring are shown in FIG. 4. Our pressure sensor has a wide range of applications in the field of wearable electronics. When applying a periodic stress and bending force to the G/GS pressure sensor, the pressure sensor shows fast and repeatable responses. High signal-to-noise ratios are observed in both cases, demonstrating the high sensitivity of our G/GS pressure sensor. Moreover, uniform performance under different types of stress will enable the application of this sensor in wearable electronic devices.

IV. CONCLUSION

The G/GS pressure sensor fabricated from graphene/graphene scrolls hybrid films on micro structured PMDS shows high sensitivity (3.5 kPa^{-1}), fast response time (within 50 ms) and excellent durability over 1000 cycles. Furthermore, tests on the application of the sensor demonstrate that it can be used to detect movement in human subjects including stress and bending force monitoring. Besides, the sensor has the advantages of easy preparation, low-cost and much flexibility, all of which are critically important for its future application in wearable electronic devices.

Supplementary materials: Preparation of graphene, statistical method of ratio about graphene scrolls, Raman spectroscopy of hybrid films, SEM image of the G/GS films coated on m-PDMS, response times of 3-, 2-layer G/GS pressure sensor and summary of recently reported piezoresistive sensors from previous work are available.

V. ACKNOWLEDGMENTS

This work was supported by the National Natural Science Foundation of China (No.21503064), Anhui Provincial Natural Science Foundation (No.1508085QE103), and the 100 Talents Program of the Chinese Academy of Sciences.

[1] J. Park, Y. Lee, J. Hong, M. Ha, Y. D. Jung, H. Lim, S. Y. Kim, and H. Ko, ACS Nano **8**, 4689 (2014).
[2] S. H. Shin, S. Ji, S. Choi, K. H. Pyo, B. Wan An, J. Park, J. Kim, J. Y. Kim, and J. U. Park, Nat. Commun. **8**, 14950 (2017).
[3] K. Takei, T. Takahashi, J. C. Ho, H. Ko, A. G. Gillies, P. W. Leu, R. S. Fearing, and A. Javey, Nat. Mater. **9**, 821 (2010).
[4] Y. Zhu, J. Li, H. Cai, Y. Wu, H. Ding, N. Pan, and X. Wang, Sensor. Actuat. B **255**, 1262 (2018).
[5] C. Wang, X. Li, E. Gao, M. Jian, K. Xia, Q. Wang, Z. Xu, T. Ren, and Y. Zhang, Adv. Mater. **28**, 6640 (2016).
[6] Y. Pang, K. Zhang, Z. Yang, S. Jiang, Z. Ju, Y. Li, X. Wang, D. Wang, M. Jian, Y. Zhang, R. Liang, H. Tian, Y. Yang, and T. L. Ren, ACS Nano **12**, 2346 (2018).
[7] H. Chen, Z. Su, Y. Song, X. Cheng, X. Chen, B. Meng, Z. Song, D. Chen, and H. Zhang, Adv. Funct. Mater. **27**, (2017).
[8] L. Q. Tao, K. N. Zhang, H. Tian, Y. Liu, D. Y. Wang, Y. Q. Chen, Y. Yang, and T. L. Ren, ACS Nano **11**, 8790 (2017).
[9] K. Xia, C. Wang, M. Jian, Q. Wang, and Y. Zhang, Nano Res. **11**, 1124 (2017).
[10] B. Zhu, Z. Niu, H. Wang, W. R. Leow, H. Wang, Y. Li, L. Zheng, J. Wei, F. Huo, and X. Chen, Small **10**, 3625 (2014).
[11] L. Zhang, G. Hou, Z. Wu, and V. Shanov, Nano LIFE **6**, 1642005 (2016).
[12] Y. Hou, D. Wang, X. M. Zhang, H. Zhao, J. W. Zha, and Z. M. Dang, J. Mater. Chem. C **1**, 515 (2013).
[13] A. Rinaldi, A. Tamburrano, M. Fortunato, and M. S. Sarto, Sensors **16**, (2016).
[14] T. Q. Trung, S. Ramasundaram, B. U. H Wang, and N. E. Lee, Adv. Mater. **28**, 502 (2016).
[15] A. S. Shaplov, D. O. Ponkratov, P. H. Aubert, E. I. Lozinskaya, C. Plesse, F. Vidal, and Y. S. Vygodskii,

DOI:10.1063/1674-0068/cjcp1907146

Chem. Commun. **50**, 3191 (2014).
[16] J. Lee, P. Lee, H. B. Lee, S. Hong, I. Lee, J. Yeo, S. S. Lee, T. S. Kim, D. Lee, and S. H. Ko, Adv. Funct. Mater. **23**, 4171 (2013).
[17] A. V. Shirinov and W. K. Schomburg, Sensor. Actuat. A **142**, 48 (2008).
[18] C. Dagdeviren, Y. Su, P. Joe, R. Yona, Y. Liu, Y. S. Kim, Y. Huang, A. R. Damadoran, J. Xia, L. W. Martin, Y. Huang, and J. A. Rogers, Nat. Commun. **5**, 4496 (2014).
[19] D. Mandal, S. Yoon, and K. J. Kim, Macromol. Rapid. Commun. **32**, 831 (2011).
[20] L. Pan, A. Chortos, G. Yu, Y. Wang, S. Isaacson, R. Allen, Y. Shi, R. Dauskardt, and Z. Bao, Nat. Commun. **5**, 3002 (2014).
[21] S. Gong, W. Schwalb, Y. Wang, Y. Chen, Y. Tang, J. Si, B. Shirinzadeh, and W. Cheng, Nat. Commun. **5**, 3132 (2014).
[22] C. Pang, G. Y. Lee, T. i. Kim, S. M. Kim, H. N. Kim, S. H. Ahn, and K. Y. Suh, Nat. Mater. **11**, 795 (2012).
[23] C. H. Mastrangelo, Z. Xia, and W. C. Tang, J. Microelectromech. S **5**, 98 (1996).
[24] S. Jung, J. Lee, T. Hyeon, M. Lee, and D. H. Kim, Adv. Mater. **26**, 6329 (2014).
[25] D. J. Cohen, D. Mitra, K. Peterson, and M. M. Maharbiz, Nano Lett. **12**, 1821 (2012).
[26] H. B. Yao, J. Ge, C. F. Wang, X. Wang, W. Hu, Z. J. Zheng, Y. Ni, and S. H. Yu, Adv. Mater. **25**, 6692 (2013).
[27] M. K. Shin, J. Oh, M. Lima, M. E. Kozlov, S. J. Kim, and R. H. Baughman, Adv. Mater. **22**, 2663 (2010).
[28] J. Kuang, Z. Dai, L. Liu, Z. Yang, M. Jin, and Z. Zhang, Nanoscale **7**, 9252 (2015).
[29] J. Park, M. Kim, Y. Lee, H. S. Lee, and H. Ko, Sci. Adv. **1**, e1500661 (2015).
[30] K. Y. Lee, H. J. Yoon, T. Jiang, X. Wen, W. Seung, S. W. Kim, and Z. L. Wang, Adv. Energy Mater. **6**, 1502566 (2016).
[31] X. Wang, Y. Gu, Z. Xiong, Z. Cui, and T. Zhang, Adv. Mater. **26**, 1336 (2014).
[32] S. C. Mannsfeld, B. C. Tee, R. M. Stoltenberg, C. V. Chen, S. Barman, B. V. Muir, A. N. Sokolov, C. Reese, and Z. Bao, Nat. Mater. **9**, 859 (2010).
[33] C. Pang, J. H. Koo, A. Nguyen, J. M. Caves, M. G. Kim, A. Chortos, K. Kim, P. J. Wang, J. B. Tok, and Z. Bao, Adv. Mater. **27**, 634 (2015).
[34] B. Su, S. Gong, Z. Ma, L. W. Yap, and W. Cheng, Small **11**, 1886 (2015).
[35] Y. Lin, X. Dong, S. Liu, S. Chen, Y. Wei, and L. Liu, ACS Appl. Mater. Inter. **8**, 24143 (2016).
[36] Y. Qin, Q. Peng, Y. Ding, Z. Lin, C. Wang, Y. Li, F. Xu, J. Li, Y. Yuan, X. He, and Y. Li, ACS Nano **9**, 8933 (2015).
[37] Y. Si, X. Wang, C. Yan, L. Yang, J. Yu, and B. Ding, Adv. Mater. **28**, 9512 (2016).
[38] S. Chun, H. Jung, Y. Choi, G. Bae, J. P. Kil, and W. Park, Carbon **94**, 982 (2015).
[39] G. Y. Bae, S. W. Pak, D. Kim, G. Lee, D. H. Kim, Y. Chung, and K. Cho, Adv. Mater. **28**, 5300 (2016).
[40] L. Lin, Y. Xie, S. Wang, W. Wu, S. Niu, X. Wen, and Z. L. Wang, ACS Nano **7**, 8266 (2013).
[41] L. Z. Sheng, Y. Liang, L. L. Jiang, Q. Wang, T. Wei, L. T. Qu, and Z. J. Fan, Adv. Funct. Mater. **25**, 6545 (2015).
[42] M. Jian, K. Xia, Q. Wang, Z. Yin, H. Wang, C. Wang, H. Xie, M. Zhang, and Y. Zhang, Adv. Funct. Mater. **27**, 1606066 (2017).
[43] W. He, G. Li, and S. Zhang, ACS Nano **9**, 4244 (2015).
[44] S. Chun, Y. Kim, H. S. Oh, G. Bae, and W. Park, Nanoscale **7**, 11652 (2015).
[45] N. Liu, A. Chortos, T. Lei, L. Jin, T. R. Kim, W. G. Bae, C. Zhu, S. Wang, R. Pfattner, X. Chen, R. Sinclair, and Z. Bao, Sci. Adv. **3** (2017).
[46] N. Lu, C. Lu, S. Yang, and J. Rogers, Adv. Funct. Mater. **22**, 4044 (2012).
[47] Y. Wei, S. Chen, X. Yuan, P. Wang, and L. Liu, Adv. Funct. Mater. **26**, 5078 (2016).
[48] Y. Wang, R. Yang, Z. Shi, L. Zhang, D. Shi, E. Wang, and G. Zhang, ACS Nano **5**, 3645 (2011).

DOI:10.1063/1674-0068/cjcp1907146